COMPARISON OF A DIFFRACTING AND A NON-DIFFRACTING CIRCULAR ACOUSTIC ARRAY

James Carneal, Marty Johnson, and Philip Gillett

Vibration and Acoustic Laboratories
Department of Mechanical Engineering
Virginia Tech

ABSTRACT

Localization of acoustic sources has been an area of research starting primarily with underwater acoustics. Recently, localization of sources in air has become a topic of interest for automatic detection, surveillance and tracking for military applications. Other application include novel teleconference devices, specifically automatic focusing on the person currently speaking. Current technology relies on free-field localization arrays, and there is a plethora of literature on array beam-forming of these arrays. This paper introduces a new technology of diffracting arrays and novel signal processing methods for characterization of these arrays and localization of acoustic sources. The theory and experimental implementation of an acoustic diffracting array (ADA) is presented, including singular value decomposition and the effect of robustness. The results indicate that ADA results in increased localization accuracy, and more directional point spread functions due to increased magnitude and phase differences compared to a free-field array.

1. INTRODUCTION

The most fundamental microphone array consists of several microphone transducers in a line, called the "line array." This simple array configuration can produce increased directivity functions by applying a "delay and sum" approach, where each of the signals is delayed by an amount which is determined by the desired directivity angle, then summed [1]. This method can be easily implemented with analog electronics. With the availability of digital signal processing methods, free-field array geometries have lead to such applications as the sniper detector, which uses a 3-D free field array to localization impulsive events based on time delay of arrival (TDOA) methods. Several methods have been offered to increase the accuracy of TDOA methods, such as cross-fixing, energy based localization, and statistical methods [2]. In the realm of teleconferencing, digital microphone array processing techniques have been used to augment the accuracy of current TDOA methods [3]. A fairly complete review of modern beamforming methods and applications can be found in Brandstein and Ward [4]. Only recently has there been interest in diffracting acoustic arrays [5,6]. Analytically, directivity of arrays mounted on hard spheres and cylinders has been shown to increase when compared with arrays in free field [7]. The advantages of a diffracting array are multiple. The diffracting array should provide increased magnitude and phase differences compared to free-field array, leading to increased accuracy and precision of directivity functions. This increased magnitude is due to surface waves forming on the outside of the diffracting object, as has been demonstrated experimentally [8]. Using this technology, the sensors themselves can be embedded into the structure of the array positioning mechanism, for example, an autonomous vehicle. The disadvantage of a diffracting array is difficulty in the determination of the directivity functions, since complex shapes will not lead to analytical solutions, but will instead require implementation of finite element models, which are computationally and time intensive. However, this can be overcome by measuring the directivity functions experimentally [9] and applying inverse filters as will be presented in this paper.

2. THEORY: ARRAY PROCESSING NEAR A DIFFRACTING OBJECT

The formulation of the array processing assumes a diffracting object in an acoustic free field, with no fluid loading, as seen in Figure 1. Microphones are embedded on or below (to incorporate mechanical protection from wind/impacts) the surface of the diffracting object. The transfer function between each source and the microphones can be formulated for the 2D case (azimuth only) or 3D case (azimuth and elevation), however this paper will concentrate only on the 2D case.

If X is the vector of sound pressures measured by I microphones at frequency ω and B is a vector of sound pressures arriving from M directions at frequency ω then X and B are related by an $I\times M$ matrix of transfer functions G which describe the way sound diffracts around the object to the microphones. Where $g_{im}(\omega)$ is the transfer function between the sound arriving from direction m and the i^{th} microphone. These equations are related as follows:

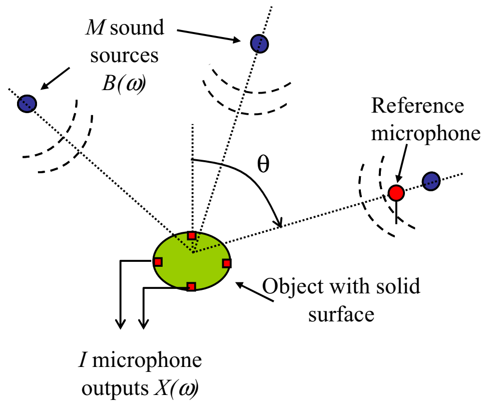

Figure 1. Acoustic Diffracting Array (ADA) consists of microphones distributed around a diffracting object.

$$X = [x_1(\omega) \quad \cdots \quad x_I(\omega)]^T \qquad \text{Eq. 1}$$

$$B = [b_1(\omega) \quad \cdots \quad b_M(\omega)]^T \qquad \text{Eq. 2}$$

$$X = GB \qquad \text{Eq. 3}$$

$$G = \begin{bmatrix} g_{1,1}(\omega) & \cdots & g_{1,M}(\omega) \\ \vdots & \ddots & \vdots \\ g_{I,1}(\omega) & \cdots & g_{I,M}(\omega) \end{bmatrix} \qquad \text{Eq. 4}$$

Currently, this matrix was measured experimentally in an anechoic chamber and used to find an optimal set of localization filters G^p (pseudo inverse of G) for sources located on the azimuth plane.

$$B \approx G^p X = \left([G^H G + \alpha * norm(G) I]^{-1} G^H\right) X \qquad \text{Eq. 5}$$

where '*H*' denotes the Hermitian or conjugate transpose, α is the conditioning factor, *norm* is the matrix norm (2) and I is the identity matrix. Note that the frequency dependence has been suppressed for simplicity. Finally, the point spread function (PSF) can be calculated as

$$PSF = BG \qquad \text{Eq. 6}$$

which is an indicator of the quality of the least mean squares curve fit performed in the pseudo-inverse calculation. For example, a perfect PSF would be a series of zeros for all arrival angles, except for the true angle of arrival, which would be non-zero. Note the PSF is a function of frequency, which is consistent with airborne acoustic array theory, i.e. the acoustic beam gets more directive as frequency increases.

To compensate for poor matrix conditioning at low frequencies, a diagonal conditioning factor of 1% of the maximum singular value was included. This will allow better inversion of the matrix, and will decrease the sensitivity to noise when the matrix condition is poor. When the matrix condition is relatively good, the conditioning factor is small relative to the singular values, and therefore has little effect.

For the current implementation of the 2D case, the measured source locations were 15^0 apart (azimuth) and the localization results were then interpolated down to a 1^0 spacing.

3. EXPERIMENTS

3.1. Experimental Setup

The experimental setup is shown in Figure 1. The array was constructed from a stiff cylindrical concrete tube with twelve microphones equally spaced (30 degrees) around the circumference at a height of half the length of the tube. The array, reference microphone, and speaker were placed in an anechoic chamber, and an array of transfer functions from the reference microphone to the twelve array microphones were measured at 15 degree increments, resulting in a 24 angles x 12 microphones x 8192 frequencies matrix.

3.2. Results

Results comparing the diffracting and non-diffracting (free-field) circular array are presented as follows. First, representative pressure and phase values as a function of sensor angle are compared for constant frequency. Second, the magnitude and phase differential between two sensors in the circular/cylindrical array, one pointing directly at the source, and the other pointing directly away from the source, is compared. Next, a singular value decomposition (SVD) of the experimental matrix is compared. The effect of the conditioning term on the array point spread function (PSF) with and without measurement noise is presented. Finally the frequencies resulting in an equivalent PSF for a free-field and diffracting array is calculated.

The pressure magnitude and phase for the free-field and diffracting array is presented in Figure 2, at a frequency of 250 Hz. As can be seen in Figure 2, the diffracting array pressure at sensor angle 0 is approximately twice the pressure of the free field array, which agrees with the fundamental physics of reflected waves from a rigid body. The diffracting array has significant magnitude differences traversing around the cylindrical array, whereas the free-field magnitude differs by <25%. As seen in the figure, the phase is comparable until the pressure wave travels past 90 degrees towards the rear of the array, where the phase angle of the diffracting array deviates from the free field by 60 degrees.

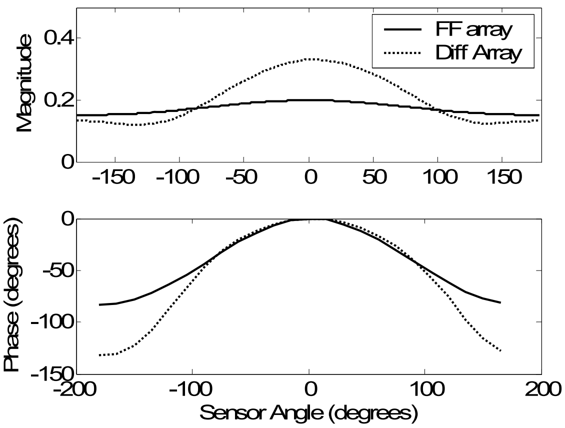

Figure 2. Normalized pressure magnitude and phase at 250 Hz for free-field (FF) and diffracting (Diff) array as a function of sensor angle relative to the source (i.e. source is at zero degrees).

The magnitude and phase differential between two sensors in the array, one pointing directly at the source, and the other pointing directly away from the source, is compared in Figure 3. As can be seen in Figure 3, the free field array shows little differential magnitude, which agrees with the acoustic propagation physics, i.e. magnitude should decay as 1/r form the source. The diffracting array presents a solid surface and creates acoustic shadowing as low as 200 Hz. Comparing the phase differential, the free field array shows typical phase delay as per acoustic propagation physics. The diffracting array presents a solid surface which results in the acoustic wave propagating along the perimeter, thereby creating a longer propagation path, and therefore more phase differential.

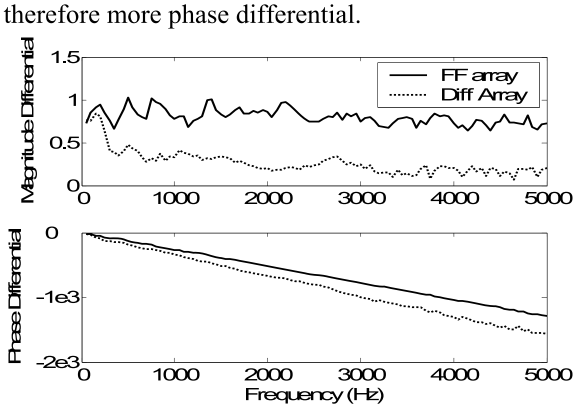

Figure 3. Magnitude and phase differential between sensor at angle=0 and sensor at angle=pi, relative to the source.

The SVD of the diffracting and free-field array measurements is presented in Figure 4. These singular values have been normalized to the first singular value. Using this method, the complexity of the system can be easily analyzed by determining how many singular values are needed to fit the data within a certain error. For example, to determine the number of singular values required to recreate the data matrix to within 90% of the original, you must include all of the singular values above -20 dB. As can be seen in Figure 4, the diffracting array has 5 singular values to above -20 dB at 250 Hz, whereas the free-field array has only three at 250 Hz. The free-field array has 5 singular values at 400 Hz, meaning that the two arrays have equivalent directivity patterns at 250 Hz for the diffracting array and 400 Hz for the free-field array.

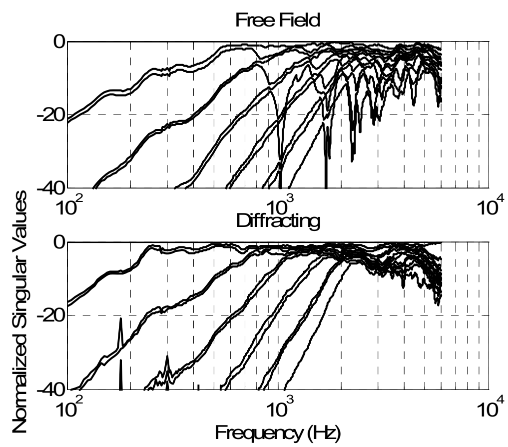

Figure 4. Normalized eigenvalues (dB) of the free-field and diffracting arrays as a function of frequency.

The second feature that is noteworthy is the minima in the singular values for the free-field array at 800-1000 Hz. These minima are a result of the wavelength being equal to the diameter of the array, leading to ambiguity in directivity.

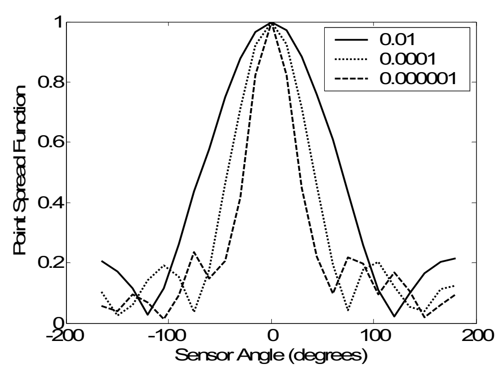

Figure 5. Effect of conditioning term on PSF of diffracting array for no noise.

The effect of the conditioning on the point spread function (PSF) of the array at 250 Hz is presented in Figure 5. As can be seen, the point spread function increases with increasing conditioning. For a low or no noise case, the conditioning should be minimized to increase the accuracy of the array. However, when there is measurement noise, either background acoustic noise, or instrumentation noise, increased matrix conditioning prevents erroneous source angle estimates as seen in Figure 6. As shown in the figure, a small amount of matrix conditioning (0.0001) can still estimate the source angle accurately for signal to noise ratio, SNR=3dB.

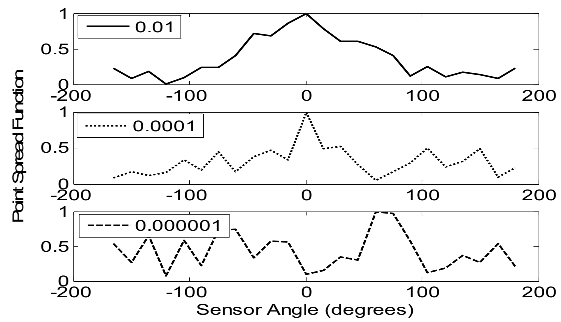

Figure 6. Effect of conditioning on PSF with SNR=3dB for diffracting array.

Finally, the main effect of the diffracting array is presented in Figure 7. The figure compares the PSF for the free-field and diffracting arrays at 400 Hz and 250 Hz, respectively, assuming no noise and a 0.01 conditioning factor. These two frequencies were chosen as to match the half-power beamwidth of the arrays. As shown in the figure, the diffracting array exhibits the same PSF as free-field array, but at a much lower frequency. Since the array sensitivity is directly a function of the wavelength relative to the array aperture, a diffracting array can be 37% smaller than a free-field array for a constant PSF.

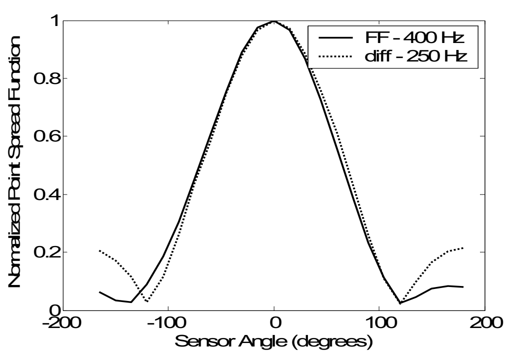

Figure 7. PSF for free-field and diffracting arrays for no noise and conditioning factor 0.01.

4. CONCLUSIONS

The theory and method of experimentally characterizing and implementing a diffracting array has been developed and verified. The addition of a conditioning term to the matrix inversion yields a robust localization methodology that is insensitive to noise. A diffracting acoustic array results in increased system complexity which results in an increased magnitude and phase differential across the array, compared to a free field array. These effects results in increased accuracy of the directivity functions for constant array size, or a smaller array size for constant directivity accuracy.

Future work will include a more strict theoretical derivation of these concepts, and extension of this technique to 3D arrays.

ACKNOWLEDGEMENTS

The authors would like to gratefully acknowledge Ausim, Inc, the DOD STTR program, and the ONR for supporting this work.

5. REFERENCES

[1] L.E. Kinsler, A. R. Frey, A. B. Coppens, J. V. Sanders, " Fundamentals of Acoustics," Wiley Press, 1999.

[2] P.E. Petila,T.W. Pirinen,A.J. Visa,T.S. Korhonen, “Comparison of three post-processing methods for acoustic localization,” in Proceedings of the SPIE Aerosense 2003 Symposium, 5090, 9-17 (2003).

[3] D.V. Rabinkin, R.J. Ranomeron, A. Dahl, J. French, J.L. Flanagan, M.H. Bianchi, “A DSP implementation of source location using microphone arrays,” J. Acoust. Soc. Am. 99, 2503-2529 (1996)

[4] M. Brandstein, D. Ward, "Microphone Arrays: Signal Processing Techniques and Applications," Springer Press, 2001.

[5] C.F. Cardoso, P. Nelson, “Directivity of Spherical Microphone Arrays”, In Proceedings of the Institute of Acoustics, 26 (2), 2001.

[6] J. Meyer, “Beamforming for a Circular Microphone Array Mounted on Spherical Shaped Objects”, J. Acoust. Soc. Am., 109 (1), 185-193 (2001).

[7] G.A. Daigle, M.R. Stinson, J.G. Ryan, ‘‘Beamforming with air-coupled surface waves around a sphere and circular cylinder,’’ J. Acoust. Soc. Am. 117, 3373-3376 (2005).

[8] M.R. Stinson, G.A. Daigle, ‘‘Surface wave formation at an impedance discontinuity,’’ J. Acoust. Soc. Am. 102, 3269-3275 (1997).

[9] M. Johnson and J. Carneal," Biologically Inspired Acoustic Direction Finding for Soldiers," Final Report submitted to AuSim, Inc. and DOD. STTR Topic A04-T013.